Natural Convection in a Porous Medium Bounded by a Long Vertical Wavy Wall and a Parallel Flat Wall

Ambrish K. Tiwari and Ashok K. Singh

Department of Mathematics, Banaras Hindu University, Varanasi, India

Reprint requests to A. K. T. or A. K. S; E-mail: aktiwaria@gmail.com or ashok@bhu.ac.in

This paper presents natural convection in a porous medium bounded by a long vertical wavy wall and a parallel wall. The shape of the wavy wall is assumed to follow a profile of cosine curve. The wall is kept at a constant heat flux while the parallel wall is kept at a constant temperature. The governing systems of nonlinear partial differential equations in their non-dimensional form are linearised by using the perturbation method in terms of amplitude and the analytical solutions for velocity and temperature fields have been obtained in terms of various parameters occurring in the model. A numerical study of the analytical solution is performed with respect to the realistic fluid air in order to illustrate the interactive influences of governing parameters on the temperature and velocity fields as well as skin friction and Nusselt number. It is found that in the case of maximum waviness (positive and negative), the velocity component along the wall has a reverse trend near the flat wall. It is observed that the parallel flow through the channel at zero waviness is greater than at maximum waviness (positive and negative) while the same trend occurs for perpendicular flow in the opposite direction. Examination of the Nusselt number shows that in the presence and absence of a heat source, the heat flows from the porous region towards the walls but in the presence of a sink, the heat flows from the walls into the porous region.

Key words: Natural Convection; Porous Medium; Wavy Wall; Perturbation Method.
2000 AMS Mathematic Subject Classification: 76R10, 76S05

1. Introduction

Transport processes as a result of natural convection inside wavy-walled channels have not been investigated widely due to geometric complexity. Literatures related to this topic are not as rich as for channels with flat walls. Natural convection heat transfer phenomenon in a porous medium bounded by geometries of irregular shape has attracted the attention of engineers and scientists from many varying disciplines such as chemical, civil, environmental, mechanical, aerospace, nuclear engineering, applied mathematics, geothermal physics, and food science. Phenomena concerned with it include the spreading of pollutants, water movement in reservoirs, thermal insulation engineering, building science, and convection in the Earth's crust etc. Geometrical complexity of such type of system affects largely the flow pattern and depends on many parameters like amplitude, wave length, phase angle, inter wall spacing etc. Each of the parameter significantly affects the hydrodynamic and thermal behaviour of the fluid inside it. These configurations are not idealities and their effects on flow phenomenon have motivated many researchers to perform experimental and analytical works.

Ostrach [1] analyzed laminar natural convection flow and heat transfer of fluids with and without heat sources in channels with constant wall temperature. Vajravelu and Sastri [2] solved free convective heat transfer in a viscous incompressible fluid confined between a long vertical wavy wall and a parallel flat wall. Shankar and Sinha [3] presented the flow generated in a viscous fluid by the impulsive motion of a wavy wall using the perturbation method about the known solution for a straight wall. Lekoudis et al. [4] analyzed compressible viscous flows past wavy walls without restricting the mean flow to be linear in the disturbance layer. Their results agree more closely with experimental data than the results obtained by using Lighthill's theory, which restricts the mean flow to be linear in the disturbance layer. The effect of small amplitude wall roughness on the minimum critical Reynolds number of a laminar boundary layer is studied by Lessen and Gangwani [5] under the assumptions

normally employed in parallel flow stability problems. By using either analytical or numerical approaches, Singh and Gholami [6], Rees and Pop [7], and Kumar [8] have solved the natural convection problem in a fluid-saturated porous media with uniform heat flux condition. The fundamental importance of convective flow in porous media has been ascertained in the recent books by Ingham and Pop [9] and Nield and Bejan [10]. Recently, several studies by Kumar et al. [11, 12], Murthy et al. [13], Kumar and Shalini [14], Misirlioglu [15] and Sultana and Hyder [16] have been reported that were concerned with the natural convection heat transfer in wavy vertical porous enclosures.

The main purpose of the present paper is to examine the free convective heat transfer and fluid flow in a porous medium bounded by a long vertical wavy wall and a parallel flat wall. The wavy wall is kept at constant heat flux while the parallel flat wall maintained at constant temperature. The solution of the governing equations has been obtained using the perturbation technique described by Nayfeh [17] in terms of the physical parameters appearing in the governing equations. Results are presented corresponding to the velocity and temperature fields as well as to the skin friction and Nusselt number for different values of the governing parameters.

2. Mathematical Formulation

Let us consider the two-dimensional laminar natural convective heat transfer flow of a viscous incompressible fluid through a porous medium bounded by a vertical wavy wall and a parallel flat wall which are maintained at constant heat flux and constant wall temperature, respectively. The properties of the fluid are assumed to be constant and isotropic except the density variation in the buoyancy term in the momentum equation. The fluid and the porous medium are in the local thermodynamic equilibrium.

The wavy surface of the wall is described in the function form as

$$y' = \varepsilon' \cos \lambda' x',$$

where the origin of the co-ordinate system is placed at the leading edge of the vertical surface, while the flat wall, which is parallel to the wavy wall, is taken at the distance $y' = d'$. The fluid oncoming to the channel is still quiescent and both the fluid and flat wall have constant temperature T_1. In this problem, the viscous and Darcy dissipation effects are neglected and the volumetric heat source/sink is constant in the energy equation.

If we define the dimensionless quantities as

$$
\begin{aligned}
&x = \frac{x'}{d'}, \quad y = \frac{y'}{d'}, \quad u = \frac{u'd'}{v}, \quad v = \frac{v'd'}{v}, \\
&\varepsilon = \frac{\varepsilon'}{d'}, \quad \theta = \frac{(T - T_1)\kappa}{qd'}, \quad P = \frac{p'd'^2}{\rho v^2}, \\
&Da = \frac{K'}{d'^2}, \quad Pr = \frac{\mu c_{\mathrm{p}}}{\kappa}, \quad \lambda = \lambda' d', \\
&G = \frac{g\beta q d'^4}{v^2 \kappa}, \quad \alpha = \frac{Qd'}{q}.
\end{aligned}
\tag{1}
$$

The dimensionless equations, governing the conservation of mass, momentum, and energy in the channel are obtained as follows (Ingham and Pop [9]):

$$\frac{\partial u}{\partial x} + \frac{\partial v}{\partial y} = 0, \tag{2}$$

$$
\begin{aligned}
u\frac{\partial u}{\partial x} + v\frac{\partial u}{\partial y} = &-\frac{\partial(P - P_s)}{\partial x} + \frac{\partial^2 u}{\partial x^2} + \frac{\partial^2 u}{\partial y^2} \\
&- \frac{u}{Da} + G\theta,
\end{aligned}
\tag{3}
$$

$$u\frac{\partial v}{\partial x} + v\frac{\partial v}{\partial y} = -\frac{\partial P}{\partial y} + \frac{\partial^2 v}{\partial x^2} + \frac{\partial^2 v}{\partial y^2} - \frac{v}{Da}, \tag{4}$$

$$Pr\left(u\frac{\partial \theta}{\partial x} + v\frac{\partial \theta}{\partial y}\right) = \frac{\partial^2 \theta}{\partial x^2} + \frac{\partial^2 \theta}{\partial y^2} + \alpha. \tag{5}$$

In the dimensionless form, the boundary conditions can be written as

$$
\begin{aligned}
&u = 0, \quad v = 0, \quad \frac{\partial \theta}{\partial y} = -1 \text{ at } y = \varepsilon\lambda x, \\
&u = 0, \quad v = 0, \quad \theta = 0 \text{ at } y = 1.
\end{aligned}
\tag{6}
$$

All the symbols used in the above equations are defined in the nomenclature.

Under the perturbation technique, let us consider the velocity and temperature fields as

$$
\begin{aligned}
&u(x,y) = u_0(y) + u_1(x,y), \quad v(x,y) = v_1(x,y), \\
&P(x,y) = P_0(x) + P_1(x,y), \\
&\theta(x,y) = \theta_0(y) + \theta_1(x,y),
\end{aligned}
\tag{7}
$$

where the first-order quantities or the perturbed parts u_1, v_1, P_1, and θ_1 are very small compared with the zeroth-order quantities or mean parts.

Using (7), (2)–(5) reduce to the following form for the zeroth-order quantities:

$$\frac{\mathrm{d}^2 u_0}{\mathrm{d}y^2} - \frac{u_0}{Da} + G\theta_0 = c, \quad \frac{\mathrm{d}^2 \theta_0}{\mathrm{d}y^2} = -\alpha, \qquad (8)$$

where, $c = \frac{\partial}{\partial x}(P_0 - P_s)$ is the constant pressure gradient term and is taken equal to zero by Ostrach [1].

For the first-order quantities we have

$$\frac{\partial u_1}{\partial x} + \frac{\partial v_1}{\partial y} = 0, \qquad (9)$$

$$u_0 \frac{\partial u_1}{\partial x} + v_1 \frac{\partial u_0}{\partial y} = -\frac{\partial P_1}{\partial x} + \frac{\partial^2 u_1}{\partial x^2} + \frac{\partial^2 u_1}{\partial y^2} \\ - \frac{u_1}{Da} + G\theta_1, \qquad (10)$$

$$u_0 \frac{\partial v_1}{\partial x} = -\frac{\partial P_1}{\partial y} + \frac{\partial^2 v_1}{\partial x^2} + \frac{\partial^2 v_1}{\partial y^2} - \frac{v_1}{Da}, \qquad (11)$$

$$Pr\left(u_0 \frac{\partial \theta_1}{\partial x} + v_1 \frac{\partial \theta_0}{\partial y}\right) = \frac{\partial^2 \theta_1}{\partial x^2} + \frac{\partial^2 \theta_1}{\partial y^2}. \qquad (12)$$

With the help of (7), the boundary conditions in (6) can be converted into the following two parts:

$$u_0 = 0, \quad \frac{\mathrm{d}\theta_0}{\mathrm{d}y} = -1 \text{ at } y = 0, \\ u_0 = 0, \quad \theta_0 = 0 \text{ at } y = 1, \qquad (13)$$

$$u_1 = -\frac{\partial u_0}{\partial y}, \quad v_1 = 0, \quad \frac{\partial \theta_1}{\partial y} = \alpha \text{ at } y = 0, \\ u_1 = 0, \quad v_1 = 0, \quad \theta_1 = 0 \text{ at } y = 1. \qquad (14)$$

2.1. Solution of the Mean Part

The zeroth-order solutions are obtained from (8) with the help of the boundary conditions in (13) in the following form:

$$\theta_0 = -\alpha \frac{y^2}{2} - y + B_0, \qquad (15)$$

$$u_0 = C_0 \mathrm{e}^{\frac{y}{\sqrt{Da}}} + D_0 \mathrm{e}^{-\frac{y}{\sqrt{Da}}} + GDa(\theta_0 - \alpha Da). \quad (16)$$

The symbols B_0, C_0, D_0 used as a constant are given in the appendix. The expression for u_0 and θ_0 are called the zero-order solutions or mean parts.

2.2. Solution Procedure for Perturbed Part

To find the solution of the first-order quantities from (9)–(12), let us introduce the stream function ψ_1 defined by

$$u_1 = -\frac{\partial \psi_1}{\partial y}, \quad v_1 = \frac{\partial \psi_1}{\partial x}. \qquad (17)$$

It is obviously clear that the continuity equation (9) is satisfied identically with the help of (17).

Using (17) into (10)–(14) and eliminating the non-dimensional pressure P_1, we have

$$u_0(\psi_{1,xxx} + \psi_{1,yyx}) - \psi_{1,x} u_0'' \\ = 2\psi_{1,xxyy} + \psi_{1,yyyy} + \psi_{1,xxxx} \\ - \frac{1}{Da}(\psi_{1,xx} + \psi_{1,yy}) - G\theta_{1,y}, \qquad (18)$$

$$Pr(u_0 \theta_{1,x} + \psi_{1,x} \theta_0') = \theta_{1,xx} + \theta_{1,yy}. \qquad (19)$$

Assuming

$$\psi_1(x,y) = \varepsilon \mathrm{e}^{\mathrm{i}\lambda x} \overline{\psi}_1(y), \quad \theta_1(x,y) = \varepsilon \mathrm{e}^{\mathrm{i}\lambda x} \overline{\theta}_1(y), \\ u_1(x,y) = \varepsilon \mathrm{e}^{\mathrm{i}\lambda x} \overline{u}_1(y), \quad v_1(x,y) = \varepsilon \mathrm{e}^{\mathrm{i}\lambda x} \overline{v}_1(y), \qquad (20)$$

and inserting into (18) and (19), we get

$$\overline{\psi}_1^{iv} - \mathrm{i}\lambda \{u_0(-\lambda^2 \overline{\psi}_1 + \overline{\psi}_1'') - u_0'' \overline{\psi}_1\} \\ - \lambda^2(2\overline{\psi}_1'' - \overline{\psi}_1 \lambda^2) - \frac{1}{Da}(\overline{\psi}_1'' - \lambda^2 \overline{\psi}_1) = G\overline{\theta}_1', \qquad (21)$$

$$\overline{\theta}_1'' - \lambda^2 \overline{\theta}_1 = \mathrm{i}\lambda Pr(u_0 \overline{\theta}_1 + \overline{\psi}_1 \theta_0'), \qquad (22)$$

where a prime denotes differentiation with respect to y.

The boundary conditions in (14) become

$$\frac{\partial \psi_1}{\partial y} = u_0', \quad \frac{\partial \psi_1}{\partial x} = 0 \text{ at } y = 0, \\ \frac{\partial \psi_1}{\partial y} = 0, \quad \frac{\partial \psi_1}{\partial x} = 0 \text{ at } y = 1. \qquad (23)$$

For small values of λ (or $\lambda^* \leq 1$), we can take

$$\overline{\psi}_1(\lambda, y) = \sum_i \lambda^i \xi_i, \quad \overline{\theta}_1(\lambda, y) = \sum_i \lambda^i \eta_i \\ (i = 0, 1). \qquad (24)$$

Inserting (24) into (21)–(22), we have obtained a set of ordinary differential equations of fourth order in term of ξ_0, ξ_1 and second order in η_0, η_1. They are not reported here for the sake of brevity. The solutions of these ordinary differential equations with their appropriate boundary conditions obtained from (23) are as follows:

$$\xi_0 = E_0 + F_0 y + G_0 \mathrm{e}^{\frac{y}{\sqrt{Da}}} + H_0 \mathrm{e}^{-\frac{y}{\sqrt{Da}}} + L_1 \theta_0, \quad (25)$$

Table 1. Values used for the parameter G, λ, α, and Da.

	— Curves —											
	1	2	3	4	5	6	7	8	9	10	11	12
G	50	50	50	50	50	50	50	50	50	100	100	100
λ	0.01	0.01	0.01	0.02	0.02	0.02	0.01	0.01	0.01	0.01	0.01	0.01
α	−5	0	5	−5	0	5	−5	0	5	−5	0	5
Da	0.01	0.01	0.01	0.01	0.01	0.01	0.1	0.1	0.1	0.01	0.01	0.01

$$\xi_1 = B_1 B_2 y B_3 e^{\frac{y}{\sqrt{Da}}} + B_4 e^{-\frac{y}{\sqrt{Da}}} - iKu_0\xi_0$$
$$- \frac{L_1 D_1}{8} y^8 - \frac{L_1 D_2}{7} y^7 - \frac{L_1 D_3}{6} y^6 - \frac{L_1 D_4}{5} y^5$$
$$+ R_1 y^4 + R_2 y^3 + R_3 y^2 + R_4 y + R_5 e^{\frac{y}{\sqrt{Da}}} \qquad (26)$$
$$+ R_6 e^{-\frac{y}{\sqrt{Da}}} + R_7 y e^{\frac{y}{\sqrt{Da}}} + R_8 y e^{-\frac{y}{\sqrt{Da}}}$$
$$- iDaL_2 C_0 y^2 e^{\frac{y}{\sqrt{Da}}} - iDaL_2 D_0 y^2 e^{-\frac{y}{\sqrt{Da}}}$$
$$+ iDaG_0 C_0 e^{\frac{2y}{\sqrt{Da}}} + iDaH_0 D_0 e^{-\frac{2y}{\sqrt{Da}}},$$

$$\eta_0 = \alpha(y-1), \qquad (27)$$

$$\eta_1 = D_1 y^7 + D_2 y^6 + D_3 y^5 + D_4 y^4 + D_5 y^3$$
$$+ D_6 y^2 + D_7 y + D_8 y e^{\frac{y}{\sqrt{Da}}} + D_9 y e^{-\frac{y}{\sqrt{Da}}} \qquad (28)$$
$$+ D_{10} e^{\frac{y}{\sqrt{Da}}} + D_{11} e^{-\frac{y}{\sqrt{Da}}} + D_{12}.$$

With the help of the above obtained solutions, the first-order quantities given by (17) along with (20) can be put in the following form:

$$u_1 = -\varepsilon[\xi'_r \cos(\lambda x) - \xi'_i \sin(\lambda x)],$$
$$v_1 = -\lambda \varepsilon[\xi_r \sin(\lambda x) - \xi_i \cos(\lambda x)], \qquad (29)$$
$$\theta_1 = \varepsilon[\eta_r \cos(\lambda x) - \eta_i \sin(\lambda x)],$$

where

$$\overline{\psi}_1 = \xi_r + i\xi_i, \quad \overline{\psi}'_1 = \xi'_r + i\xi'_i,$$
$$\overline{\theta}_1 = \eta_r + i\eta_i, \quad \overline{\theta}'_1 = \eta'_r + i\eta'_i. \qquad (30)$$

The expressions for the first-order velocity u_1, v_1 and the first-order temperature θ_1 have been obtained with the help of (25)−(28).

3. Skin Friction and Nusselt Number at the Walls

The shear stress τ_{xy} at any point of the fluid in the non-dimensional form is given by

$$\tau_{xy} = \frac{\partial u}{\partial y} + \frac{\partial v}{\partial x}.$$

Using above equation, the skin friction τ_ω at the wavy wall ($y = 0$) and τ_1 at the flat wall ($y = 1$) are obtained as

$$\tau_\omega = u'_0(0) + Re[\varepsilon e^{i\lambda x} u''_0(0) + \varepsilon e^{i\lambda x} \overline{u}'_1(0)]$$
$$= S_1 - \varepsilon[S_2 \cos(\lambda x) - S_3 \sin(\lambda x)], \qquad (31)$$

$$\tau_1 = u'_0(1) + Re[\varepsilon e^{i\lambda x} \overline{u}'_1(1)]$$
$$= S_4 - \frac{\varepsilon}{Da}[S_5 \cos(\lambda x) - S_6 \sin(\lambda x)]. \qquad (32)$$

The Nusselt number Nu_ω at the wavy wall ($y = 0$) and Nu_1 at the flat wall ($y = 1$) in the dimensionless form are obtained as

$$Nu_\omega = \theta'_0(0) + Re[\varepsilon e^{i\lambda x} \theta''_0(0) + \varepsilon e^{i\lambda x} \overline{\theta}'_1(0)]$$
$$= -1 + \varepsilon[\alpha \cos(\lambda x) - N_1 \sin(\lambda x)], \qquad (33)$$

$$Nu_1 = \theta'_0(1) + Re[\varepsilon e^{i\lambda x} \overline{\theta}'_1(1)]$$
$$= -(\alpha + 1) + \varepsilon[\alpha \cos(\lambda x) - N_2 \sin(\lambda x)]. \qquad (34)$$

4. Results and Discussion

The expressions for the mean part u_0, θ_0 and the perturbed part u_1, v_1, θ_1 have been obtained in terms of physical parameters G, ε, λ, α, Pr, and Da. The involvement of many parameters in a study not only makes the computational works a formidable task but it also makes it difficult to incorporate a systematic parametric presentation. Thus we set $Pr = 0.71$ corresponding to the realistic fluid air, $\varepsilon = 0.002$, and focus our attention on numerical computations for different values of G, λ, α, and Da as given in Table 1.

Graphical representations of the mean part as well as the perturbed part of the velocity and the temperature profiles of air are shown in Figures 1−5 for the above data. Figure 1 describes the behaviour of the mean part u_0 of the velocity between vertical walls. Close examination of it reveals that in the presence of a source, the velocity profiles take a parabolic shape but reverse shape in the presence of a sink. The point of maxima on the curves get shifted away from the parallel flat
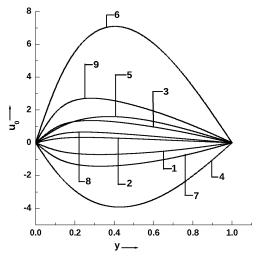
Fig. 1. Zeroth-order velocity profile.

Fig. 2. Zeroth-order temperature profile.

wall ($y = 1$) as Grashof number and Darcy number increase. Although in the absence of source/sink, the velocity profiles are almost flat while assuming parabolic shapes due to overshooting in velocity near the flat wall ($y = 0$) as value of Grashof number and Darcy number increase. It is clear from curves $(3, 9)$ that the velocity increases with the Grashof number G for $\alpha = 5$ but reverse flow occurs for $\alpha = -5$ (see curves $1, 7$). In the absence of source/sink ($\alpha = 0$), the velocity near the flat wall ($y = 0$) increases with an increase in Grashof number G but near the flat wall ($y = 1$) the velocity is approximately same as Grashof number G increases. On the examination of curves $(3, 6)$ and $(2, 5)$, one can reveal that the velocity is an increasing function of G and Da in the presence and absence of source/sink while in the presence of sink, it is an increasing function of G and Da in the opposite direction shown by the curves $(1, 4)$.

The behaviour of the mean temperature θ_0 is shown in Figure 2, from which it is clear that in the absence of a heat source ($\alpha = 0$), the mean temperature is a linearly decreasing function of y (curves $2, 5, 8$) while in the presence of a heat source ($\alpha = 5$), the mean temperature is increasing from its value at the wall $y = 0$ to a maximum temperature at around $y = 0.1$ and then decreasing steadily its value up to $y = 1$ (curves $3, 6, 9$). In the presence of heat sink ($\alpha = -5$), the behaviour of the mean temperature is exact opposite of that observed in the presence of source (curves $1, 4, 7$). Further, we observed that there is no significant effect of λ, G, and Da on the mean temperature θ_0 for all values of α.
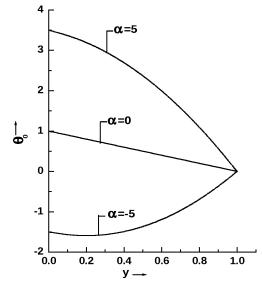
4.1. Presentation of the First-Order Solution

Figures 3, 4, and 5 represent the perturbed part (first-order solution) of the velocity components u_1, v_1 and temperature θ_1, respectively, in the channel for three cases of the waviness of the wavy wall ($y = 0$). They are as follows: (i) maximum positive at $\lambda x = 0$, (ii) zero at $\lambda x = \frac{\pi}{2}$, and (iii) maximum negative at $\lambda x = \pi$. The description of the first-order solution at different types of waviness is as follows.

The effect of maximum waviness on the first-order velocity component u_1 is shown in Figure 3a and it indicates that in the presence of a heat sink, the velocity component u_1 increases near the wavy wall and then by decreasing becomes zero at $y = 0.70$ approximately and thereafter reverse flow occurs. We observed from the curves $(1, 4)$ that with increasing Darcy number Da the velocity component u_1 increases in two third of the channel and this behaviour is reversed in the presence or absence of heat source as shown in the curves $(3, 6)$ or $(2, 5)$, respectively. This behaviour is reversed in the other one third of the channel. On analysing the curves $(1, 7)$ for $\alpha < 0$, we found that with the increase of the Grashof number G, the velocity component u_1 increases in two third of the channel and this behaviour is reversed when $\alpha \geq 0$ (see curves $3, 9$ and $2, 8$). However, in the other one third of the channel this behaviour of the velocity component u_1 with G is reversed.
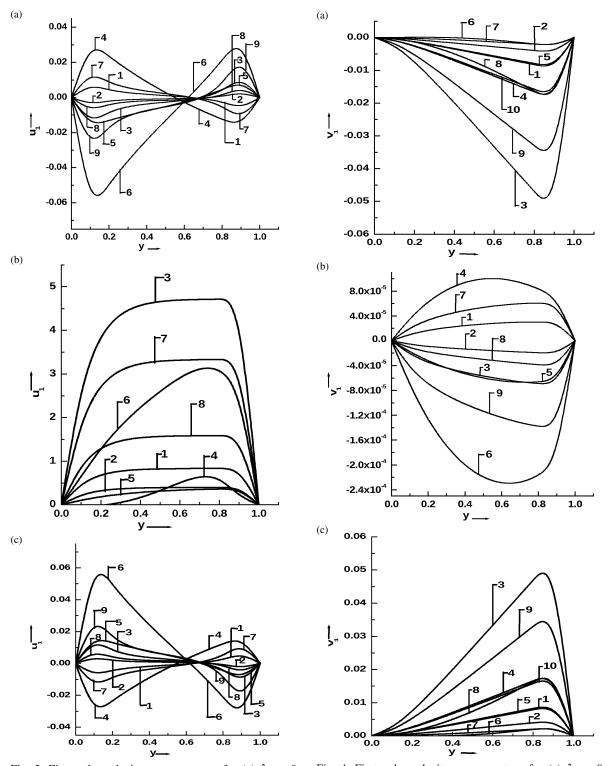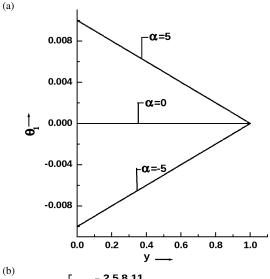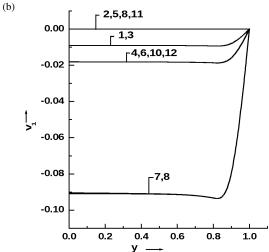
(a)

(a)

(b)

(b)

(c)

(c)

Fig. 3. First-order velocity component u_1 for (a) $\lambda x = 0$, (b) $\lambda x = \frac{\pi}{2}$, and (c) $\lambda x = \pi$.

Fig. 4. First-order velocity component v_1 for (a) $\lambda x = 0$, (b) $\lambda x = \frac{\pi}{2}$, and (c) $\lambda x = \pi$.
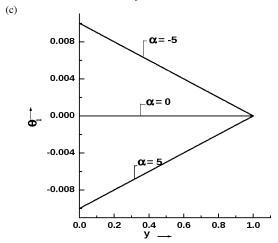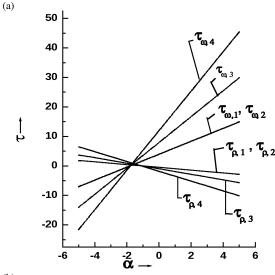
(a)

(b)

(c)

Fig. 5. First-order temperature profiles θ_1 for (a) $\lambda x = 0$, (b) $\lambda x = \frac{\pi}{2}$, and (c) $\lambda x = \pi$.

Figure 3b, showing the perturbed velocity component u_1 for zero waviness, indicates that it increases in the present of a heat source (curves 2, 3 and 5, 6). The effect of Darcy number is also to increase it (curves 1, 7 and 2, 8). For maximum negative waviness (Fig. 3c), we found that reversed effects are observed for source and sink parameter. The effects of the parameters which appear in it are reversed of all the results found for maximum positive waviness.

It is observed from Figure 4a that the velocity component v_1 is enhanced by an increase in the Darcy number Da in the reverse direction by the curves (3, 9) and (1, 7) in the presence of heat source and sink, respectively, while in the absence of heat source/sink it decreases. In the presence of heat source/sink, the velocity component v_1 is an increasing function of λ and Da by curves (3, 6) and (1, 4) while in the absence of heat source/sink, the velocity component v_1 is also an increasing function of λ and Da in the opposite direction (see curves 2 and 5).

It is observed from the curves (1, 4, 7, and 10) of Figure 4b that for $\alpha < 0$, the velocity component v_1 is an increasing function of λ, G, and Da while for $\alpha \geq 0$, the reverse effect can be seen by the curves (3, 6, 9, and 12) and (2, 5, 8, and 11). Close observation of Figure 4c shows that the behaviour of the velocity component v_1 in case of maximum negative waviness is almost reverse to that of positive maximum waviness.

The behaviour of the perturbed temperature θ_1 with changes in α is shown in Figure 5 according to three cases of waviness of the wavy wall. Figure 5a showing the perturbed part of temperature for $\lambda x = 0$, which indicates that in the absence of a heat source/sink, the perturbed temperature is zero (curves 2, 5, 8) while in the presence of a heat source, it is a linearly decreasing function of y (curves 3, 6, 9). In the presence of a heat sink, the behaviour of the perturbed temperature is exactly opposite of that observed in the presence of a source (curves 1, 4, 7). The parameters λ, G, and Da have also negligible effect on the perturbed temperature for all values of α. For zero waviness, we observe from Figure 5b that the perturbed temperature is almost the same up to $y = 0.8$ of the channel and then increases in the remaining part of the channel. The behaviours of the perturbed temperature at maximum negative waviness are shown in Figure 5c. The effect of source and sink are just reversed corresponding to the maximum positive waviness but for absence of source/sink, both cases have the same effect.
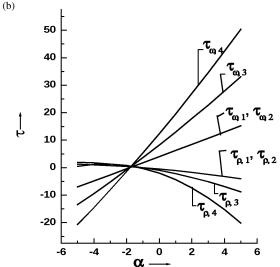
(a)

(b)

Fig. 6. Total skin-friction at the wall for (a) $\lambda x = 0$, (b) $\lambda x = \frac{\pi}{2}$. The curves are drawn based on the following data:

| | — Curves — | | | |
	1	2	3	4
G	50	50	100	100
λ	0.01	0.02	0.01	0.01
Da	0.01	0.01	0.01	0.02

The curves of skin friction are shown in Figures 6a,b only for the maximum positive waviness ($\lambda x = 0$) and zero waviness ($\lambda x = \frac{\pi}{2}$) because the perturbed part is much smaller than the mean part and the curves for maximum negative waviness ($\lambda x = \pi$) almost coincide with Figure 6a.

It is observed that the skin friction at the channel walls is a linear function of the heat source parame-
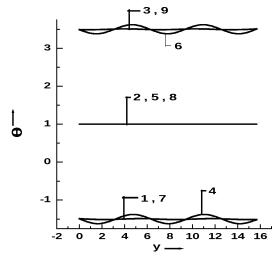

Fig. 7. Temperature of the wavy wall.

ter α and the skin friction at the wall $y = 0$ increases with the heat source parameter α while the reverse is true at the other wall $y = 1$ in both types of channel walls. The skin friction is an increasing function of the Grashof number G and the Darcy number Da by the curves $(3, 4)$ at the wall $y = 0$ while at $y = 1$ it decreases with an increase in G and Da. It is clear from curves $(1, 2)$ that the skin friction is unaffected by frequency parameter λ in both cases. On comparing the skin friction for both types of waviness of the wall at $y = 0$ and $y = 1$, it is observed that it is greater in the case when the channel has a maximum positive waviness than in the case when the channel has zero waviness.

The temperature profiles of the wavy wall are shown in Figure 7. It is observed that the temperature of the wavy wall is a linear function of the phase λx for all values of G and it becomes oscillatory when the value of the Darcy number Da increases in the presence of source ($\alpha = 5$) and sink ($\alpha = -5$). In the absence of source/sink ($\alpha = 0$), the wavy wall temperature linearly varies as function of G and Da as the perturbed part is much smaller than the mean part.

Lastly in Table 2, the values of the Nusselt number at the channel wall ($y = 1$) are given only for maximum positive waviness and zero waviness for different values of G, λ, and Da. The Nusselt numbers for maximum negative waviness are approximately the same as for maximum positive waviness. It can be seen from this table that the Nusselt number at the flat wall ($y = 1$) in both types of waviness decreases with G, α, and Da and this decrease being least significant for Da than G and most significant for α. The effects of λ on the Nus-

Table 2. Numerical values of dimensionless Nusselt number for $Pr = 0.71$.

	Values of Nusselt number at the flat wall ($y = 1$)							
	For $\lambda x = 0$				For $\lambda x = \pi/2$			
α	$G = 50$ $\lambda = 0.01$ $Da = 0.01$	$G = 50$ $\lambda = 0.02$ $Da = 0.01$	$G = 100$ $\lambda = 0.01$ $Da = 0.01$	$G = 100$ $\lambda = 0.01$ $Da = 0.02$	$G = 50$ $\lambda = 0.01$ $Da = 0.01$	$G = 50$ $\lambda = 0.02$ $Da = 0.01$	$G = 100$ $\lambda = 0.01$ $Da = 0.01$	$G = 100$ $\lambda = 0.01$ $Da = 0.02$
−5	3.97996	3.96992	3.96992	3.94984	3.36137	3.36137	2.72274	1.43997
−4	2.98555	2.97915	2.97914	2.96630	2.59119	2.59119	2.18238	1.36204
−3	1.99038	1.98677	1.98677	1.97954	1.77005	1.77005	1.54010	1.07933
−2	0.99439	0.99278	0.99278	0.98957	0.89795	0.89795	0.79591	0.59184
−1	−0.00240	−0.00280	−0.00280	−0.00360	−0.02509	−0.02509	−0.05019	−0.1004
0	−0.99999	−0.99999	−0.99999	−0.99999	−0.99910	−0.99910	−0.99820	−0.9974
1	−1.99840	−1.99880	−1.99880	−1.99960	−2.02406	−2.02406	−2.04813	−2.0992
2	−2.99760	−2.99921	−2.99921	−3.00242	−3.09998	−3.09998	−3.19996	−3.4058
3	−3.99761	−4.00113	−4.00123	−4.00845	−4.22685	−4.22685	−4.45371	−4.9172
4	−4.99842	−5.00485	−5.00485	−5.01770	−5.40468	−5.40468	−5.80937	−6.6333
5	−6.00004	−6.01008	−6.01008	−6.03016	−6.63347	−6.63347	−7.26694	−8.5542

selt number for maximum positive waviness ($\lambda x = 0$) on increasing the value of λ is that the Nusselt number has approximately the same value for $\alpha \leq 0$ and decreased value for $\alpha > 0$ while for zero waviness ($\lambda x = \frac{\pi}{2}$), the Nusselt number is exactly the same for all values of α. Also, when the heat source/sink parameter α takes positive increasing values, the Nusselt number at the flat wall ($y = 1$) in both types of waviness becomes negative, which means physically that heat flows from the porous region towards the walls. However, when the heat source/sink parameter α takes negative increasing values, the Nusselt number at the flat wall ($y = 1$) in both types of waviness is positive, which indicates physically that heat flows from the walls into the porous region.

5. Conclusions

The two-dimensional natural convective heat transfer flow of a viscous and incompressible fluid through a porous medium bounded by a vertical wavy wall and a parallel flat wall which are maintained at constant heat flux and constant wall temperature, respectively, has been studied. The governing equations in non-dimensional form are linearised by using the perturbation technique. An analytical solution for the mean part as well as the perturbed part has been obtained and using them, detailed analysis of velocity and temperature fields are presented in graphical form for various values of the parameters. We have also discussed the surface skin-friction coefficient as well as the Nusselt numbers at the flat wall ($y = 1$) and temperature of the wavy wall ($y = 0$). The important fact of this study is a comparison among three types of waviness of the wall. It is observed that the parallel flow through a channel

at zero waviness is greater than at maximum waviness (positive and negative) while the same trend occurs for perpendicular flow in reverse direction.

Nomenclature

c_p	Specific heat at constant pressure defined in (1)
d'	Distance between both walls
Da	Darcy number defined in (1)
G	Grashof number or free convection parameter defined in (1)
g	Acceleration due to gravity
K'	Permeability of the porous medium
Nu	Nusselt number
P	Fluid pressure
P'	Dimensionless fluid pressure defined in (1)
Pr	Prandtl number defined in (1)
q	Rate of heat transfer
Q	Source/sink parameter
T	Fluid temperature
T_1	Temperature of the flat wall
u, v	Dimensionless velocity components along x and y-axis, respectively
u', v'	Velocity components along x and y-axis, respectively
x, y	Dimensionless Cartesian coordinates
x', y'	Cartesian coordinates

Greek symbols

α	Dimensionless source/sink parameter defined in (1)
β	Volumetric coefficient of thermal expansion
ε	Dimensionless amplitude parameter
ε'	Amplitude parameter
θ	Dimensionless fluid temperature defined in (1)
κ	Thermal conductivity
λ	Dimensionless frequency parameter defined in (1)
λ'	Frequency parameter
μ	Dynamic viscosity
ν	Kinematic viscosity
ρ	Fluid density
τ	Skin friction or dimensionless shear stress
ψ_1	Dimensionless stream function

Subscripts

0 Zero-order quantity   1 First-order quantity   s Static fluid ω Wavy wall   p Flat wall

Appendix

$$A_1 = iPr[\alpha C_0(\sqrt{Da}+Da)+\alpha D_0(Da-\sqrt{Da})+\alpha L_1(B_0-Da)+G_0(\sqrt{Da}-\alpha Da)+H_0(\sqrt{Da}+\alpha Da)],$$

$$A_2 = iPr\left[2\alpha\left\{\sqrt[3]{Da}(C_0+D_0)+L_1\left(-\frac{\alpha}{120}+\frac{B_0}{6}-\frac{1}{24}\right)+DaL_1\left(-\frac{\alpha}{6}+B_0+\frac{1}{2}\right)\right\}\right.$$
$$+(\alpha+1)\left\{\frac{E_0}{2}+\frac{F_0}{6}+DaG_0e^{\frac{1}{\sqrt{Da}}}-DaH_0e^{-\frac{1}{\sqrt{Da}}}+L_1\left(-\frac{\alpha}{180}+\frac{B_0}{12}-\frac{1}{40}\right)\right\}$$
$$\left.-2\alpha\left\{\frac{E_0}{2}+\frac{F_0}{24}+\sqrt[3]{Da}(G_0e^{\frac{1}{\sqrt{Da}}}+H_0e^{-\frac{1}{\sqrt{Da}}})+L_1\left(-\frac{\alpha}{1260}+\frac{B_0}{60}-\frac{1}{240}\right)\right\}\right]-A_1,$$

$$B_0 = 1+\alpha/2, \quad B_1 = -B_3-B_4-P_1, \quad B_2 = (B_4-B_3)\frac{1}{\sqrt{Da}}-P_3, \quad B_3 = \frac{\sqrt{Da}(P_4-P_3)+M_1B_4}{M_2},$$

$$B_4 = \frac{(\sqrt{Da}M_2+1)(P_3-P_4)-M_2(P_1+P_3-P_2)}{2M_1M_2+(M_1-M_2)\frac{1}{\sqrt{Da}}}, \quad C_0 = \frac{L_1(B_0-\alpha DaM_2)e^{-\frac{1}{\sqrt{Da}}}}{(M_4-M_3)},$$

$$D_0 = \frac{L_1(B_0-\alpha DaM_1)e^{\frac{1}{\sqrt{Da}}}}{(M_3-M_4)}, \quad D_1 = \frac{\alpha iL_2}{252}, \quad D_2 = \frac{2iL_2}{90}, D_3 = \frac{iL_1Pr-\alpha iL_2-2iB_0L_2}{40},$$

$$D_4 = \frac{\alpha iL_2-2iL_1B_0Pr-\alpha 2iF_0Pr-2iL_2}{24}, \quad D_5 = \frac{iB_0L_2-\alpha iDaL_2-iF_0Pr-\alpha iPr+iL_2}{6},$$

$$D_6 = \frac{1}{2}(\alpha iDaL_2-iB_0L_2-iE_0Pr), \quad D_7 = iDaL_2-iDaB_0L_2+A_1, \quad D_8 = \alpha iDaPr(C_0-G_0),$$

$$D_9 = \alpha iDaPr(D_0H_0), \quad D_{10} = -iDaPr(\alpha C_0+G_0)-i\sqrt[3]{Da}Pr(\alpha 2C_0+G_0),$$

$$D_{11} = iDaPr(H_0-\alpha D_0)+i\sqrt[3]{Da}Pr(H_0+\alpha 2D_0), \quad D_{12} = -iDaB_0L_2+A_2,$$

$$E_0 = -G_0-H_0-L_1B_0, F_0 = \frac{(H_0-G_0+C_0-D_0)}{\sqrt{Da}}, \quad G_0 = \frac{H_0M_1+(C_0-D_0-L_1\sqrt{Da})-\alpha L_1\sqrt{Da}}{M_2},$$

$$H_0 = \frac{\left(\frac{\alpha L_1}{2}\right)(2\sqrt{Da}M_2+M_4)-\left(\sqrt{Da}M_2+e^{\frac{1}{\sqrt{Da}}}\right)S_1}{2M_1M_22(M_1-M_2)\frac{1}{\sqrt{Da}}}, L_1 = DaG, \quad L_2 = \alpha DaGPr, \quad L_3 = i\alpha DaL_1,$$

$$M_1 = 1-e^{-\frac{1}{\sqrt{Da}}}, \quad M_2 = 1-e^{\frac{1}{\sqrt{Da}}}, \quad M_3 = 1+e^{-\frac{1}{\sqrt{Da}}}, \quad M_4 = 1+e^{\frac{1}{\sqrt{Da}}},$$

$$N_1 = \left(D_7+D_8+D_9+\frac{D_{10}}{\sqrt{Da}}-\frac{D_{11}}{\sqrt{Da}}-\alpha\right),$$

$$N_2 = \left(7D_1+6D_2+5D_3+4D_4+3D_5+2D_6+D_7+\left(D_8+\frac{D_8}{\sqrt{Da}}+\frac{D_{10}}{\sqrt{Da}}\right)e^{\frac{1}{\sqrt{Da}}}\right.$$
$$\left.+\left(D_9-\frac{D_9}{\sqrt{Da}}-\frac{D_{11}}{\sqrt{Da}}\right)e^{-\frac{1}{\sqrt{Da}}}\right),$$

$$P_1 = R_5+R_6+iDa(C_0G_0+D_0H_0),$$

$$P_2 = -L_1\left(\frac{D_1}{8}+\frac{D_2}{7}+\frac{D_3}{6}+\frac{D_4}{5}\right)+R_1+R_2+R_3+R_4+(R_5+R_8-C_0L_3)e^{\frac{1}{\sqrt{Da}}}+(R_6+R_7-D_0L_3)e^{-\frac{1}{\sqrt{Da}}},$$

$$P_3 = -L_1(D_{10}+D_{11}+D_{12}),$$

$$P_4 = -L_1(D_1+D_2+D_3+D_4+D_5+D_6+D_7+(D_8+D_{10})e^{\frac{1}{\sqrt{Da}}}+(D_9+D_{11})e^{-\frac{1}{\sqrt{Da}}}+D_{12}),$$

$$R_1 = \frac{L_1}{4}(\alpha L_3-D_5), \quad R_2 = \frac{1}{6}(-4F_0L_3+2L_3L_1-2D_6L_1),$$

$$R_3 = -L_1(iDa(F_0+\alpha E_0)+(B_0-1)L_3+\frac{1}{2}(D_7+A_1)),$$

$$R_4 = -2iDaE_0L_1-2i\sqrt{Da}(G_0D_0-H_0C_0)-2iDa(B_0-1)L_1^2-D_{12}L_1,$$

$$R_5 = 2i(DaC_0E_0-\sqrt[3]{Da}(C_0F_0-G_0L_1)+\alpha Da^2L_1(G_0-C_0)+(B_0-1)DaC_0L_1)-\left(\frac{D_{10}}{\sqrt{Da}}-DaD_8\right)L_1,$$

$$R_6 = 2i(DaD_0E_0+\sqrt[3]{Da}(D_0F_0-H_0L_1)+\alpha Da^2L_1(H_0-D_0)+(B_0-1)DaD_0L_1)-\left(\frac{D_{11}}{\sqrt{Da}}-DaD_9\right)L_1,$$

$$R_7 = 2\mathrm{i}(DaC_0F_0 + \alpha\sqrt[3]{Da}L_1(C_0 - G_0)) - \sqrt{Da}D_8L_1, \quad R_8 = 2\mathrm{i}(DaD_0F_0 + \alpha\sqrt[3]{Da}L_1(H_0 - G_0)) + \sqrt{Da}D_9L_1,$$

$$S_1 = \left(\frac{C_0}{\sqrt{Da}} - \frac{D_0}{\sqrt{Da}} - L_1\right), \quad S_2 = \left(\frac{G_0}{\sqrt{Da}} + \frac{H_0}{\sqrt{Da}} - \alpha L_1\right),$$

$$S_3 = \frac{B_3}{Da} + \frac{B_4}{Da} - 2Da\left(\frac{C_0}{Da} + \frac{D_0}{Da} - \alpha L_1\right)^2$$
$$+ \frac{1}{Da}(2R_3Da + R_5 + R_6 + 2R_7\sqrt{Da} - 2R_8\sqrt{Da} - 2L_2C_0Da^2 - 2L_2D_0Da^2),$$

$$S_4 = \frac{1}{\sqrt{Da}}\left(C_0\mathrm{e}^{\frac{1}{\sqrt{Da}}} - D_0\mathrm{e}^{-\frac{1}{\sqrt{Da}}}\right) - L_1(\alpha+1), \quad S_5 = \left(G_0\mathrm{e}^{\frac{1}{\sqrt{Da}}} + H_0\mathrm{e}^{-\frac{1}{\sqrt{Da}}} - L_1\alpha Da\right),$$

$$S_6 = (B_3 + R_5 + 2R_7\sqrt{Da} + R_7 - L_2C_0Da(2Da + 4\sqrt{Da} + 1))\mathrm{e}^{\frac{1}{\sqrt{Da}}}$$
$$+ (B_4 + R_6 - 2R_8\sqrt{Da} - R_8 - L_2D_0Da(2Da - 4\sqrt{Da} + 1))\mathrm{e}^{-\frac{1}{\sqrt{Da}}}.$$

[1] S. Ostrach, N.A.S.A. Tech. Note No. **2863** (1952).

[2] K. Vajravelu and K. S. Sastri, J. Fluid Mech. **86**, 365 (1978).

[3] P. N. Shankar and U. N. Sinha, J. Fluid Mech. **77,** 243 (1976).

[4] S. G. Lekoudis, A. H. Nayfeh, and W. S. Saric, Phys. Fluids **19**, 514 (1976).

[5] M. Lessen and S. T. Gangwani, Phys. Fluids, **19**, 510 (1976).

[6] A. K. Singh and H. R. Gholami, Rev. Roum. Sci. Techn. Mech. Appl. **35**, 337 (1990).

[7] D. A. Rees and I. Pop, ASME J. Heat Transf. **117**, 547 (1995).

[8] B. V. R. Kumar, Numer. Heat Transf. **A 37**, 493 (2000).

[9] D. B. Ingham and I. Pop, Transport Phenomena in Porous Media, Pergamon, Oxford 2002.

[10] D. A. Nield and A. Bejan, Convection in Porous Media, Springer-Verlag, New York 2006.

[11] B. V. R. Kumar, P. Singh, and P. V. S. N. Murthy, ASME J. Heat Transf. **119**, 848 (1997).

[12] B. V. R. Kumar, P. V. S. N. Murthy, and P. Singh, Int. J. Numer. Meth. Fluids **28**, 633 (1998).

[13] P. V. S. N. Murthy, B. V. R. Kumar, and P. Singh, Numer. Heat Transf. **A 31**, 207 (1997).

[14] B. V. R. Kumar, and Shalini, Int. J. Eng. Sci. **41**, 1827 (2003).

[15] A. Misirlioglu, A. C. Baytes, and I. Pop, Int. J. Heat Mass Transf. **48**, 1840 (2005).

[16] Z. Sultana and M. N. Hyder, Int. Commun. Heat Mass Transf. **34**, 136 (2007).

[17] A. H. Nayfeh, Perturbation Methods, Willey-Interscience, New York 1973.